Inorg. Chem. **2003**, *42*, 8690–8701

Coordination Chemistry of a New Cofacial Binucleating Macropolycycle Derived from 1,4,7-Triazacyclononane

Lorenzo Tei,[†,‡] Massimiliano Arca,[†] M. Carla Aragoni,[†] Andrea Bencini,[§] Alexander J. Blake,[‡] Claudia Caltagirone,[†] Francesco A. Devillanova,[†] Patrizia Fornasari,[§] Alessandra Garau,[†] Francesco Isaia,[†] Vito Lippolis,*[,†] Martin Schröder,*[,‡] Simon J. Teat,[||] and Barbara Valtancoli[§]

Dipartimento di Chimica Inorganica ed Analitica, Università degli Studi di Cagliari, Complesso Universitario di Monserrato, S.S. 554 Bivio per Sestu, 09042 Monserrato (CA), Italy, School of Chemistry, The University of Nottingham, University Park, Nottingham NG7 2RD, U.K., Dipartimento di Chimica, Università di Firenze, Polo Scientifico, Via della Lastruccia 3, 50019 Sesto Fiorentino, Florence, Italy, and CLRC Daresbury Laboratory, Keckwick Lane, Daresbury, Warrington WA4 4AD, U.K.

Received May 13, 2003

We have prepared and characterized a new phenol-based compartmental ligand (H_2L) incorporating 1,4,7-triazacyclononane ([9]aneN_3), and we have investigated its coordination behavior with Cu^{II}, Zn^{II}, Cd^{II}, and Pb^{II}. The protonation constants of the ligand and the thermodynamic stabilities of the 1:1 and 2:1 (metal/ligand) complexes with these metal ions have been investigated by means of potentiometric measurements in aqueous solutions. The mononuclear [M(L)] complexes show remarkably high stability suggesting that, along with the large number of nitrogen donors available for metal binding, deprotonated phenolic functions are also involved in binding the metal ion. The mononuclear complexes [M(L)] show a marked tendency to add a second metal ion to afford binuclear species. The formation of complexes $[M_2(H_2L)]^{4+}$ occurs at neutral or slightly acidic pH and is generally followed by metal-assisted deprotonation of the phenolic groups to give $[M_2(HL)]^{3+}$ and $[M_2(L)]^{2+}$ in weakly basic solutions. The complexation properties of H_2L have also been investigated in the solid state. Crystals suitable for X-ray structural analysis were obtained for the binuclear complexes $[Cu_2(L)](BF_4)_2 \cdot {}^1/_2$MeCN (**1**), $[Zn_2(HL)](ClO_4)_3 \cdot {}^1/_2$MeCN (**2**), and $[Pb_2(L)](ClO_4)_2 \cdot 2$MeCN (**4**). In **1** and **2**, the phenolate O-donors do not bridge the two metal centers, which are, therefore, segregated each within an N_5O-donor compartment. However, in the case of the binuclear complex $[Pb_2(L)](ClO_4)_2 \cdot 2$MeCN (**4**), the two Pb^{II} centers are bridged by the phenolate oxygen atoms with each metal ion sited within an N_5O_2-donor compartment of L^{2-}, with a Pb···Pb distance of 3.9427(5) Å.

Introduction

The rational design and synthesis of ligand systems capable of accommodating two or more metal centers in close proximity and in predetermined spatial arrangements is an active area of research.[1−3] Indeed, polynuclear complexes, in which cation−cation interactions can be tuned via variation functionality in the ligand structure, find applications as models for important metallobiosites,[4] as catalysts,[5] and in the investigation of the mutual influence of proximal metal centers on the electronic, magnetic, and redox properties of such systems.[5,6] In this respect, great attention has been focused on the use of phenol-based compartmental macrocycles,[7,8] since their homo- and hetero-binuclear complexes generally show two metal ions bound and situated in close proximity through the bridging phenolic oxygen donor atoms.

* Authors to whom correspondence should be addressed. E-mail: lippolis@unica.it (V.L.). Phone: +39 0706754467 (V.L.). Fax: +39 0706754456 (V.L.); E-mail: m.schroder@nottingham.ac.uk (M.S.). Phone: +44 1159513490 (M.S.). Fax: +44 1159513563 (M.S.).

[†] Università degli Studi di Cagliari.

[‡] The University of Nottingham.

[§] Università di Firenze.

[||] Daresbury Laboratory.

(1) (a) Gavrilova, A. L.; Quin, C. J.; Sommer, R. D.; Rheingold, A. L.; Bosnich, B. *J. Am. Chem. Soc.* **2002**, *124*, 1714−1722. (b) Spencer, D. J. E.; Johnson, B. J.; Tolman, W. B. *Org. Lett.* **2002**, *4*, 1391−1393. (c) Roder, J. C.; Meyer, F.; Konrad, M.; Sandhofner, S.; Kaifer, E.; Pritzkow, H. *Eur. J. Org. Chem.* **2001**, 4479−4487. (d) Abe, K.; Matsufuji, K.; Ohba, M.; Okawa, H. *Inorg. Chem.* **2002**, *41*, 4461−4467. (e) Siegfried, L.; Kaden, T. A.; Meyer, F.; Kircher, P.; Pritzkow, H. *J. Chem. Soc., Dalton Trans.* **2001**, 2310−2315.

(2) (a) Adams, H.; Clunas, S.; Fenton, D. E.; Spey, S. E. *J. Chem. Soc., Dalton Trans.* **2002**, 441−448. (b) Formica, M.; Fusi, V.; Giorgi, L.; Micheloni, M.; Palma, P.; Pontellini, R. *Eur. J. Org. Chem.* **2002**, 402−404. (c) Fry, F. H.; Moubaraki, B.; Murray, K. S.; Spiccia, L.; Warren, M.; Skelton, B. W.; White, A. H. *J. Chem. Soc., Dalton Trans.* **2003**, 866−871. (d) Beckmann, U.; Bill, E.; Weyhermuller, T.; Wieghardt, K. *Inorg. Chem.* **2003**, *42*, 1045−1056. (e) Beckmann, U.; Brooker, S.; Depree, C. V.; Ewing, J. D.; Moubaraki, B.; Murray, K. S. *J. Chem. Soc., Dalton Trans.* **2003**, 1308−1313.

10.1021/ic0345065 CCC: $25.00
Published on Web 11/21/2003

Scheme 1

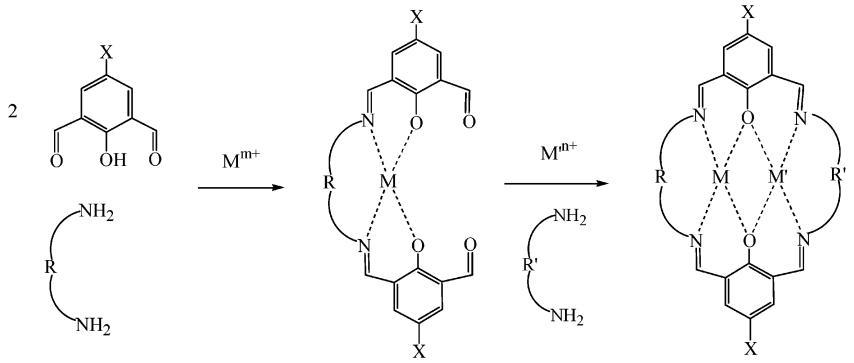

The synthesis of compartmental macrocyclic ligands is normally achieved by a template Schiff-base condensation between 2,6-diformyl-4-substituted phenols and 1,*n*-diamines (Scheme 1). Changing the structural features of the 1,*n*-diamines connecting the two phenolic units has recently been the main objective of research aimed either at increasing the binding selectivity of these systems or at introducing differentiation between the sets of donor atoms at the two metal binding sites.[7−9] However, less attention has been focused on the reduced form of the phenol-based compartmental macrocycles,[10] although interesting studies in this regard have been reported by Martell and co-workers,[11−15] who have found that metal complexes of the Schiff-base form of these diphenol macrocycles exhibit different coordination properties from those of the corresponding amine form.

In a recent communication,[16] we have reported the synthesis and coordination chemistry of Cd^{II} and Y^{III} with a new phenol-based compartmental system (H_2L^1 in Scheme 2) in which, for the first time, a preformed macrocycle has been introduced as part of the lateral chains connecting the two *p*-cresol units to afford a large binucleating cofacial macropolycycle. In H_2L^1, the particular binding properties of phenol-based compartmental macrocycles have been combined with those of [9]aneN_3 (1,4,7-triazacyclononane) to afford a ligand characterized by two large adjacent chambers, each with a potential N_5O_2 donor set capable of accommodating, in close proximity, two metal ions with large ionic radii. The ability of H_2L^1 to form homo-binuclear complexes in which the two metal centers are bridged by the phenolate oxygen atoms has been shown to depend on the nature of the metal ion. In the binuclear Cd^{II} complex $[Cd_2(L^1)]^{2+}$ the *p*-cresolate O-donors are not shared by the two metal centers, which are each bound within an independent N_5O-donating compartment. However, bridging *p*-cresolate oxygen donors are observed in the binuclear Y^{III} complex $[Y_2(L^1)(OH)]^{3+}$.[16] It is important to note that the smaller Cd^{II} ion seldom adopts

(3) (a) Lee, D.; Hung, P. L.; Spingler, B.; Lippard, S. J. *Inorg. Chem.* **2002**, *41*, 521−531. (b) Chartres, J. D.; Lindoy, L. F.; Meehan, G. V. *Coord. Chem. Rev.* **2001**, *216−217*, 249−286. (c) Fontecha, J. B.; Goetz, S.; McKee, V. *Angew. Chem., Int. Ed.* **2002**, *41*, 4553−4556. (d) Cromie, S.; Launay, F.; McKee, V. *Chem. Commun.* **2001**, 1918−1919.

(4) (a) Fenton, D. E.; Okawa, H. *Chem. Ber./Recl.* **1997**, *130*, 433−442. (b) Fenton, D. E. *Chem. Soc. Rev.* **1999**, *28*, 159−168. (c) Gao, J.; Martell, A. E.; Motekaitis, R. J. *Inorg. Chim. Acta* **2001**, *325*, 164−170. (d) Buchler, S.; Meyer, E.; Kaifer, E.; Pritzkow, H. *Inorg. Chim. Acta* **2002**, 337, 371−386. (e) He, C.; Lippard, S. J. *Inorg. Chem.* **2001**, *40*, 1414−1420. (f) Westerheide, L.; Müller, F. K.; Than, R.; Krebs, B.; Dietrich, J.; Schindler, S. *Inorg. Chem.* **2001**, *40*, 1951−1961. (g) Suzuki, M.; Furutachi, H.; Okawa, H. *Coord. Chem. Rev.* **2000**, *200−202*, 105−129. (h) Liable-Sands, L. M.; Incarvito, C.; Rheingold, A. L.; Quin, C. J.; Gavrilova, A. L.; Bosnich, B. *Inorg. Chem.* **2001**, *40*, 2147−2155.

(5) (a) Lehn, J.-M. *Pure Appl. Chem.* **1980**, *52*, 2441−2459. (b) Lehn, J.-M. *Supramolecular Chemistry. Concepts and Perspectives*; VCH: Weinheim, Germany, 1995. (c) Roder, J. C.; Meyer, F.; Kaifer, E. *Angew. Chem., Int. Ed.* **2002**, *41*, 2304−2306.

(6) (a) Kahn, O. *Struct. Bonding* **1987**, *68*, 89−167. (b) Kahn, O. *Adv. Inorg. Chem.* **1995**, *43*, 179−254. (c) Gou, S.; Quian, M.; Yu, Z.; Duan, C.; Sun, X.; Huang, W. *J. Chem. Soc., Dalton Trans.* **2001**, 3232−3237. (d) Tolman, W. B. *Acc. Chem. Res.* **1997**, *30*, 227−237. (e) Furutachi, H.; Ishida, A.; Miyasaka, H.; Fukita, N.; Ohba, M.; Okawa, H.; Koikawa, M. *J. Chem. Soc., Dalton Trans.* **1999**, 367−372.

(7) (a) Okawa, H.; Furutachi, H.; Fenton, D. E. *Coord. Chem. Rev.* **1998**, *174*, 51−75. (b) Alexander, V. *Chem. Rev.* **1995**, *95*, 273−342. (c) Guerriero, P.; Vigato, P. A.; Fenton, D. E.; Hellier, P. C. *Acta Chem. Scand.* **1992**, *46*, 1025−1046. (d) Fraser, C.; Ostrander, R.; Rheingold, A. L.; White, C.; Bosnich, B. *Inorg. Chem.* **1994**, *33*, 324−337. (e) McCollun, D. G.; Hall, L.; White, C.; Ostrander, R.; Rheingold, A. L.; Whelan, J.; Bosnich, B. *Inorg. Chem.* **1994**, *33*, 924−933.

(8) (a) Zanello, P.; Tamburini, S.; Vigato, P. A.; Mazzocchin, G. A. *Coord. Chem. Rev.* **1987**, *77*, 165−273. (b) Atkins, A. J.; Black, D.; Blake, A. J.; Marin-Becerra, A.; Parsons, S.; Ruiz-Ramirez, L.; Schröder, M. *J. Chem. Soc., Chem. Commun.* **1996**, 457−464. (c) Fenton, D. E.; Okawa, H. *Perspectives on Bioinorganic Chemistry*; JAI Press: London, 1993; Vol. 2, pp 81−138. (d) Kahwa, I. A.; Folkes, S.; Williams, D. J.; Ley, S. V.; O'Mahoney, C. A.; McPherson, G. L. *J. Chem. Soc., Chem. Commun.* **1989**, 1531−1533.

(9) (a) Adams, H.; Fenton, D. E.; Haque, S. R.; Heath, S. L.; Ohba, M.; Okawa, H.; Spey, S. E. *J. Chem. Soc., Dalton Trans.* **2000**, 1849−1856. (b) Casellato, U.; Tamburini, S.; Tomasin, P.; Vigato, P. A.; Aime, S.; Barge, A.; Motta, M. *Chem. Commun.* **2000**, 145−146. (c) Yonemura, M.; Okawa, H.; Ohba, M.; Fenton, D. E.; Thompson, L. K. *Chem. Commun.* **2000**, 817−818. (d) Furutachi, H.; Fujinami, S.; Suzuki, M.; Okawa, H. *J. Chem. Soc., Dalton Trans.* **1999**, 2197−2203. (e) Kita, S.; Furutachi, H.; Okawa, H. *Inorg. Chem.* **1999**, *38*, 4038−4045.

(10) (a) Mandal, S. K.; Thompson, L. K.; Nag, K.; Charland, J. P.; Gabe, E. J. *Inorg. Chem.* **1987**, *26*, 1391−1395. (b) Okawa, H.; Tadokoro, M.; Aratake, Y.; Ohba, M.; Shindo, K.; Mitsumi, M.; Koikawa, M.; Tomono, M.; Fenton, D. E. *J. Chem. Soc., Dalton Trans.* **1993**, 253−258. (c) Adams, H.; Clunas, S.; Fenton, D. E.; Spey, S. E. *J. Chem. Soc., Dalton Trans.* **2003**, 625−630.

(11) Shangguan, G.; Martell, A. E.; Zhang, Z.; Reibenspies, J. H. *Inorg. Chim. Acta* **2000**, *299*, 47−58.

(12) Kong, D.; Reibenspies, J.; Martell, A. E.; Motekaitis, R. J. *Inorg. Chim. Acta* **2001**, *324*, 35−45.

(13) He, H.; Martell, A. E.; Motekaitis, R. J.; Reibenspies, J. H. *Inorg. Chem*. **2000**, *39*, 1586−1592.

(14) Wang, J.; Martell, A. E.; Motekaitis, R. J. *Inorg. Chim. Acta* **2001**, *322*, 47−55.

(15) (a) Kong, D.; Martell, A. E.; Motekaitis, R. J.; Reibenspies, J. H. *Inorg. Chim. Acta* **2001**, *317*, 243−251. (b) Wang, J.; Kong, D.; Martell, A. E.; Motekatis, R. J.; Reibenspies, J. H. *Inorg. Chim. Acta* **2001**, *324*, 194−202.

(16) Tei, L.; Blake, A. J.; Devillanova, F. A.; Garau, A.; Lippolis, V.; Wilson, C.; Schröder, M. *Chem. Commun.* **2001**, 2582−2583.

Scheme 2. (i) $TsN(CH_2)_2$, MeCN, reflux 3 h; (ii), conc. H_2SO_4, 110 °C 72 h; (iii), amberlite IEA-416; (iv), 2,6-diformyl-4-methylphenol, MeOH, reflux 2 h; (v), $NaBH_4/NaBH_3CN$, MeOH, r.t. 30 h

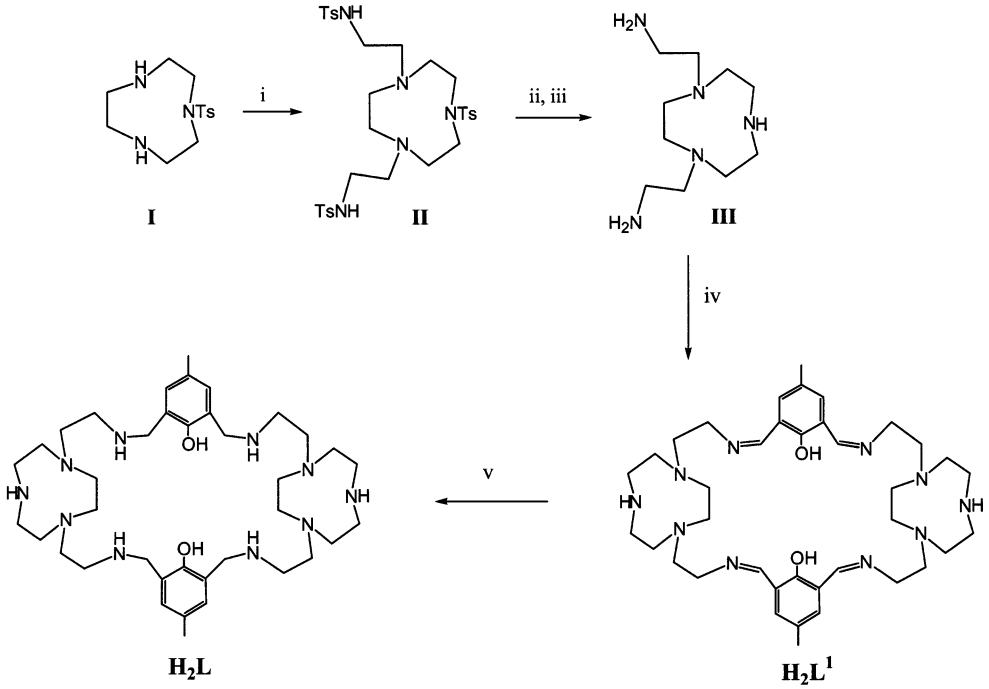

coordination numbers higher than six in these and related systems, while the larger Y^{III} ion normally shows higher coordination numbers of 8−9 in its complexes.

We were interested in discovering whether the coordination behavior of H_2L^1 is determined by the rigidity imposed by the four azomethine linkages to the macrocyclic framework: for this reason we chemically reduced the imine bonds in H_2L^1 to afford H_2L, a new and more flexible cofacial macropolycycle. Significantly, unlike H_2L^1, the binding behavior of H_2L can be studied potentiometrically in water solution since there are no C═N bonds in H_2L which could undergo hydrolysis. We report herein the coordinative properties of H_2L both in solution and in the solid state toward a series of metal ions (Cu^{II}, Zn^{II}, Cd^{II}, and Pb^{II}) which are characterized by different stereochemical preferences.

Experimental Section

Microanalytical data were obtained using a Fisons EA CHNS-O instrument ($T = 1000$ °C). ^{13}C and ^1H NMR spectra were recorded on a Varian VXR300 spectrometer (operating at 75.4 MHz). EI (electron impact) mass spectra were measured using a V6 Autospec V67070E spectrometer. Electrospray and FAB (fast atom bombardment) mass spectra were obtained by the EPSRC National Mass Spectrometry Service at the University of Swansea. UV−vis spectra were recorded at 25 °C using a Varian model Cary 5 UV−vis−NIR spectrophotometer, and a Perkin-Elmer 1600 spectrometer was used for recording FTIR spectra (KBr disks). 1-(*p*-Tolylsulfonyl)-1,4,7-triazacyclononane,[17] *N*-(*p*-tolylsulfonyl)-aziridine,[18] and 2,6-diformyl-4-methyl-phenol[19] were prepared as described in the literature. All starting materials were obtained from Aldrich Chemical Co. and were used without further purification.

Caution! The Zn^{II} and Pb^{II} complexes of H_2L were isolated in the solid state as perchlorate salts. Although we worked with these complexes on a small scale without any incident, the unpredictable behavior of perchlorate salts necessitates extreme care in their handling.

Synthesis of 1-(*p*-Tolylsulfonyl)-4,7-bis(2-aminoethyl-*N*-*p*-tolylsulfonyl)-1,4,7- triazacyclononane (II). 1-(*p*-Tolylsulfonyl)-1,4,7-triazacyclononane (**I**) (2.36 g, 8.7 mmol) was dissolved in MeCN (100 cm^3), and the resulting solution heated to reflux under nitrogen. Subsequently, a solution of *N*-(*p*-tolylsulfonyl)-aziridine (3.46 g, 17.5 mmol) in acetonitrile (50 cm^3) was added over a period of 2 h. The resulting mixture was heated under reflux for a further 2 h. After cooling, the solvent was removed under reduced pressure to yield a pale yellow solid (5.67 g, 8.36 mmol, yield 96.1%). Anal. Found (Calcd for $C_{31}H_{43}N_5O_6S_3$): C, 54.64 (54.92); H, 6.23 (6.39); N, 10.14 (10.33); S, 14.10 (14.19). FAB mass spectrum (3-NOBA matrix), *m*/*z* found: 700.3 and 678.3 for 700.9 [M + Na^+] and 677.9 [M], respectively. ^1H NMR (300 MHz, 298 K, $CDCl_3$): δ_H 1.55 (N*H*, 2H, broad singlet), 2.40 (ArCH_3, 6H, s), 2.44 (ArCH_3, 3H, s), 2.68−2.71 (NCH_2 ring, 8H, m), 2.85 (NCH_2CH_2N arms, 4H, m), 2.96 (ArNCH_2 ring, 4H, t, $J = 5.67$ Hz), 3.17 (ArNCH_2 arms, 4H, m), 7.65 (Ar*H*, 2 H, d, $J = 8.21$ Hz), 7.31 (Ar*H*, 2 H, d, $J = 8.21$ Hz), 7.77 (Ar*H*, 4 H, d, $J = 7.86$ Hz), 7.27 (Ar*H*, 4 H, d, $J = 7.86$ Hz). ^{13}C NMR (75.4 MHz, 298 K, $CDCl_3$): δ_C 21.48, 41.48, 54.25, 55.99, 56.23, 57.01, 127.24, 129.71, 136.91, and 144.24.

Synthesis of 1,4-Bis (2-aminoethyl)-1,4,7-triazacyclononane (III). 1-(*p*-Tolylsulfonyl)-4,7-bis(2-aminoethyl-N-*p*-tolylsulfonyl)-1,4,7-triazacyclononane (**II**) (0.320 g, 1.23 mmol) was dissolved in concentrated H_2SO_4 (40 cm^3) and heated to 110 °C under nitrogen atmosphere for 72 h. After cooling, the dark solution was added over a period of 1 h to a mixture of diethyl ether and ethanol. The solid formed was filtered, washed with ether, and dissolved in H_2O. The aqueous solution was then passed through an Amberlite IRA 416 column (30 g) activated with a 1 M solution of NaOH. The

(17) Sessler, J. L.; Sibert, J. W.; Lynch, V. *Inorg. Chem.* **1990**, *29*, 4143−4146.
(18) Bencini, A.; Fabbrizzi, L.; Poggi, A. *Inorg. Chem.* **1981**, *20*, 2544−2549.
(19) Lindoy, L. F.; Meehan, G. V.; Svenstrup, N. *Synthesis* **1998**, 1029−1032.

solvent was removed under reduced pressure to yield a colorless oil (1.01 g, 4.33 mmol, yield 91.7%). Anal. Found (Calcd for $C_{10}H_{25}N_5 \cdot H_2O$): C, 51.41 (51.47); H, 11.55 (11.66); N, 29.82 (30.01). EI mass spectrum, *m*/*z* found: 185.2, 168.2, 142.1, and 128.1 for 185.3 [$M^+ - CH_2NH_2$], 169.2 [$M^+ - CH_2NH_2 - NH_2$], 141.1 [$M^+ - CH_2CH_2NH_2 - CH_2NH_2$], and 127.1 [$M^+ - 2CH_2$-$CH_2NH_2$], respectively. ^{1}H NMR (300 MHz, 298 K, $CDCl_3$): δ_H 2.08 (NH_2, 4H, br), 2.56−2.65 (NCH_2, 16 H, m), 2.74 (CH_2NH$_2$, 4 H, t, J = 5.83 Hz). ^{13}C NMR (75.4 MHz, 298 K, $CDCl_3$): δ_C 40.34 (NCH$_2$*C*H$_2$NH$_2$), 46.78 (*C*H$_2$HN*C*H$_2$), 52.21, 53.72 (N*C*H$_2$ ring), 61.29 (N*C*H$_2$CH$_2$NH$_2$).

Synthesis of H_2L^1. A solution of 4,7-bis(2-aminoethyl)-1,4,7-triazacyclononane (**III**) (0.15 g, 0.64 mmol) in MeOH (10 mL) was added dropwise to a solution of 2,6-diformyl-4-methylphenol (0.105 g, 0.64 mmol) in MeOH (20 mL). The resulting solution was heated under reflux for 2 h. After cooling, the solvent volume was reduced, petroleum ether (40−60 °C) was added, and the yellow solid which formed was filtered off and dried under reduced pressure (0.182 g, 0.265 mmol, yield 82.6%). Anal. Found (Calcd for $C_{38}H_{58}N_{10}O_2$): C, 66.15 (66.44); H, 8.39 (8.51); N, 20.24 (20.39). FAB mass spectrum (3-NOBA matrix) *m*/*z*, found: 709, 687 for [M + Na^+] and [M], respectively. ^{1}H NMR (300 MHz, 298 K, $CDCl_3$): δ_H 2.30 (ArCH_3, 6 H, s), 2.55−2.72 (NCH_2, 32 H, m), 3.47 (CH_2N═C, 8 H, m), 7.36 (Ar*H*, 4 H, s), 8.36 (N═C*H*, 4 H, s). ^{13}C NMR (75.4 MHz, 298 K, $CDCl_3$): δ_C 20.36, 47.18, 51.99, 53.95, 57.40, 58.40, 118.44, 125.40, 126.98, 130.75, 131.72, 157.09, and 165.59. IR (KBr disk) ν(cm^{-1}): 2925s, 2852s, 1637s and 1600s ($\nu_{C=N}$), 1458s, 1384s, 1260m, 1101m, 1033m, and 804m.

Synthesis of $H_2L \cdot 4H_2O$. $NaBH_3CN$ (0.146 g, 2.33 mmol) and $NaBH_4$ (0.088 g, 2.33 mmol) were added in small portions to a solution of H_2L^1 (0.400 g, 0.582 mmol) in MeOH (50 cm^3). The resulting mixture was stirred at room temperature for 30 h; the solvent was then removed under reduced pressure, and the resulting light brown solid was recovered with H_2O (5 cm^3). The solution was basified to pH 14 with NaOH and extracted with ethyl acetate (6 × 50 cm^3). The collected organic fractions were dried over Na_2SO_4 and filtered. After removal of the solvent, the resulting pale yellow solid was dried under reduced pressure (0.282 g, 0.406 mmol, yield 69.8%). Anal. Found (Calcd for $C_{38}H_{66}N_{10}O_2 \cdot 4H_2O$): C, 60.05 (59.50); H, 9.39 (9.72); N, 18.74 (18.26). FAB mass spectrum (3-NOBA matrix), *m*/*z* found: 718, 696 for [M + Na^+] and [M + H^+], respectively. ^{1}H NMR (300 MHz, 298 K, $CDCl_3$): δ_H 2.19 (NCH_2, 8 H, m), 2.26 (ArCH_3, 6 H, s), 2.53−2.66 (NCH_2, 40 H, m), 6.75 (Ar*H*, 4 H, s). ^{13}C NMR (75.4 MHz, 298 K, $CDCl_3$): δ_C 20.54 (Ar*C*H$_3$), 46.33 and 47.89 (*C*H$_2$HN*C*H$_2$), 50.59, 50.96, and 53.05 (N*C*H$_2$), 57.59 (N*C*H$_2$Ar), 124.30, 127.15, 128.32, and 154.02, (*C* benzene ring). IR (KBr disk) ν(cm^{-1}): 3205m, 2922m, 2858m, 1480s, 1385s, 1260m, 1120m, 868m, and 810m.

General Procedures for the Synthesis of Complexes. A mixture of $H_2L \cdot 4H_2O$ (30 mg, 0.039 mmol) and the appropriate metal salt (0.078 mmol) in MeCN (10 cm^3) was stirred at room temperature for 4 h. Crystalline solids were obtained by slow evaporation-diffusion of Et_2O vapor into concentrated solutions of the complexes in MeCN.

$[Cu_2(L)](BF_4)_2 \cdot {}^1/_2$MeCN (1). Anal. Found (Calcd for $C_{39}H_{65.5}B_2$-$Cu_2F_8N_{10.5}O_2$): C, 46.35 (46.19); H, 6.71 (6.51); N, 14.55 (14.50). Electrospray mass spectrum, *m*/*z*: 907 for [$^{63}Cu_2(L)(BF_4)]^+$. IR spectrum (KBr disk) ν(cm^{-1}): 3310m, 3244m, 2928m, 2860m, 1475s, 1384s, 1260m, 1084s, 880m, 805m.

$[Zn_2(HL)](ClO_4)_3 \cdot {}^1/_2$MeCN (2). Anal. Found (Calcd for $C_{42}H_{71}$-$Cl_3N_{12}O_{14}Zn_2$): C, 41.78 (41.86); H, 6.10 (5.94); N, 14.11 (13.95). Electrospray mass spectrum, *m*/*z*: 924 and 412 for $[Zn_2(L)(ClO_4)]^+$ and $\{[Zn_2(L)]_{1/2}\}^+$, respectively. IR spectrum (KBr disk) ν(cm^{-1}): 3240m, 2922m, 2870m, 1475s, 1386m, 1260m, 1148s, 1120s, 1190s, 875m, 797m, 630s.

$[Cd_2(L)](NO_3)_2 \cdot 2$MeCN (3). Anal. Found (Calcd for $C_{42}H_{70}$-$Cd_2N_{14}O_8$): C, 44.51 (44.88); H, 6.59 (6.28); N, 17.05 (17.45). Electrospray mass spectrum, *m*/*z*: 980 and 459 for $[^{112}Cd_2(L)(NO_3)]^+$ and $\{[^{112}Cd_2(L)]_{1/2}\}^+$, respectively. IR spectrum (KBr disk) ν(cm^{-1}): 3264m, 2920m, 2851m, 1472m, 1384s, 1006w, 802w.

$[Pb_2(L)](ClO_4)_2 \cdot 2$MeCN (4). Anal. Found (Calcd for $C_{42}H_{70}$-$Cl_2N_{12}O_{10}Pb_2$): C, 36.58 (36.34); H, 5.41 (5.08); N, 12.33 (12.11). Electrospray mass spectrum, *m*/*z*: 1307, 1207, and 554; for $[^{207}Pb_2(HL)(ClO_4)_2]^+$, $[^{207}Pb_2(L)(ClO_4)]^+$, and $\{[^{207}Pb_2(L)]_{1/2}\}^+$, respectively. IR spectrum (KBr disk) ν(cm^{-1}): 3210m, 2920m, 2860m, 1470s, 1386m, 1300m, 1260m, 1110s, 1090s, 870m, 795m, 628s.

Potentiometric Measurements. All the pH metric measurements were carried out at 298.1 K in degassed 0.1 M Me_4NCl aqueous solutions, using equipment and procedures which have already been described.[20] The combined Ingold 405 S7/120 electrode was calibrated as a hydrogen concentration probe by titrating known amounts of HCl with CO_2-free Me_4NOH solutions and determining the equivalent point by Gran's method[21] which allows one to determine the standard potential $E°$, and the ionic product of water (pK_w = 13.83(1) at 298.1 K in 0.1 M Me_4NCl). At least three potentiometric titrations were performed for each system in the pH range 2.5−11.0. A standard ligand concentration ([H_2L] = 1.0 × 10^{-3} M) was adopted for all complexation experiments, while metal concentration was varied from [M^{2+}] = 0.8 × 10^{-3} M to 1.8 × 10^{-3} M. The relevant emf data were analyzed using the computer program HYPERQUAD.[22] All titrations were treated either as single sets or as separate entities for each system without significant variation in the values of the determined constants. In the HYPERQUAD program, the sum of the weighted square residuals on the observed emf values is minimized. The weights were derived from the estimated errors in emf (0.2 mV) and titrant volume (0.002 cm^3). The most probable chemical model was selected by following a strategy based on the statistical inferences applied to the variance of the residuals, σ^2. The sample standard deviation should be 1, in the absence of systematic errors and when a corrected weighting scheme is used. However, the agreement is considered good for standard deviation values smaller than 3 ($\sigma^2 < 9$). Values of σ^2 lower than 6 were obtained for all the refined equilibrium models in the present works. If more than one model gave acceptable σ^2, the reliability of the proposed speciation models was checked by performing *F* tests at the 0.05 confidence level, using the method reported in ref 23 for two different proposed models, A and B. Assuming that the minimum value of the sample variance, σ_A^2, has been reached for the proposed model A, an alternative model B, which supplies a value of the variance σ_B^2 was rejected if $\sigma_B^2/\sigma_A^2 > F$, where σ_A and σ_B are given directly by data treatment with the HYPERQUAD[22] program. The *F* values were taken from ref 23a. For all the systems investigated, this method leads to define univocally one acceptable system.

Spectrophotometric Measurements. Spectrophotometric titrations were carried out at 298.1 K in 0.1 M Me_4NCl aqueous solutions, using a Perkin-Elmer Lambda 9 spectrophotometer. HCl

(20) Bazzicalupi, C.; Bencini, A.; Fusi, V.; Giorgi, C.; Paoletti, P.; Valtancoli, B. *Inorg. Chem.* **1998**, *37*, 941−948.
(21) Gran, G. *Analyst (Cambridge, U.K.)* **1952**, *77*, 661−663.
(22) Gans, P.; Sabatini, A.; Vacca, A. *Talanta* **1996**, *43*, 1739−1753. Gans, P.; Sabatini, A.; Vacca, A. *J. Chem. Soc., Dalton Trans.* **1985**, 1195−1200.
(23) (a) Hamilton, W. C. *Statistics in Phisycal Chemistry*; The Ronald Press Company: New York, 1964. (b) Bologni, L.; Sabatini, A.; Vacca, A. *Inorg. Chim. Acta* **1983**, *69*, 71−75.

Table 1. Selected Crystallographic Data for the Single Crystal Structure Determinations of $[H_8L](ClO_4)_6 \cdot 8H_2O$, $[Cu_2(L)](BF_4)_2 \cdot {}^1/_2MeCN$ (**1**), $[Zn_2(HL)](ClO_4)_3 \cdot {}^1/_2MeCN$ (**2**), and $[Pb_2(L)](ClO_4)_2 \cdot 2MeCN$ (**4**)

	$[H_8L](ClO_4)_6 \cdot 8H_2O$	$[Cu_2(L)](BF_4)_2 \cdot {}^1/_2MeCN$	$[Zn_2(HL)](ClO_4)_3 \cdot {}^1/_2MeCN$	$[Pb_2(L)](ClO_4)_2 \cdot 2MeCN$
formula	$C_{38}H_{88}Cl_6N_{10}O_{34}$	$C_{39}H_{65.5}B_2Cu_2F_8N_{10.5}O_2$	$C_{42}H_{71}Cl_3N_{12}O_{14}Zn_2$	$C_{42}H_{70}Cl_2N_{12}O_{10}Pb_2$
M/g mol^{-1}	1441.88	1014.22	1205.20	1388.38
cryst syst	monoclinic	orthorhombic	monoclinic	triclinic
space group	$P2_1/n$ (No.14)	$Fdd2$ (No. 43)	$P2_1/n$ (No. 14)	$P\bar{1}$ (No. 2)
a/Å	13.457(2)	28.064(3)	12.433(2)	10.0027(7)
b/Å	8.282(2)	48.112(5)	13.414(2)	10.7873(8)
c/Å	29.319(5)	15.996(2)	15.575(2)	12.5946(9)
α/deg				102.819(2)
β/deg	102.796(4)		100.734(2)	106.811(2)
γ/deg				97.918(2)
U/Å^3	3186.5(11)	21598(4)	2552.1(6)	1238.44(15)
T/K	150(2)	150(2)	120(2)	150(2)
Z	2	16	2	1
D_c/g cm^{-3}	1.503	1.269	1.568	1.862
μ/mm^{-1}	0.368	0.855	1.173	6.964
unique reflns, R_{int}	6237, —	3964, 0.058	4425, 0.063	5566, 0.031
obsd reflns	2259 [$F_o \geq 4\sigma(F_o)$]	3295 [$F_o \geq 4\sigma(F_o)$]	3437 [$F_o \geq 4\sigma(F_o)$]	5295 [$F_o \geq 4\sigma(F_o)$]
R1,[a] wR2[b] (all data)	0.0796, 0.232	0.0766, 0.218	0.0608, 0.170	0.0368, 0.0795

[a] $R1 = \sum||F_o| - |F_c||/\sum|F_o|$. [b] $wR2 = \{\sum[w(F_o^2 - F_c^2)^2]/\sum[w(F_o^2)^2]\}^{1/2}$.

and Me_4NOH were used to adjust the pH that was measured using a Metrohm 713 pH meter. The pK_a values for deprotonation of the complex $[Pb_2(H_2L)]^{4+}$ were obtained from the spectrophotometric titration curve by data treatment with the HYPERQUAD[22] program.

Crystallography. A summary of the crystal data and refinement details for the compounds discussed in this chapter is given in Table 1. Data for $[H_8L](ClO_4)_6 \cdot 8H_2O$ and $[Pb_2(L)](ClO_4)_2 \cdot 2MeCN$ were collected on a Bruker SMART APEX CCD area detector diffractometer equipped with an Oxford Cryosystems open-flow cryostat[24] using graphite-monochromated Mo Kα radiation ($\lambda = 0.71073$ Å). Data for $[Cu_2(L)](BF_4)_2 \cdot {}^1/_2MeCN$ were collected on a similarly equipped Bruker SMART 1K CCD area detector diffractometer using synchrotron radiation ($\lambda = 0.6861$ Å) on station 9.8 of the Daresbury SRS. Data for $[Zn_2(HL)](ClO_4)_3 \cdot {}^1/_2MeCN$ were collected on a similarly equipped Nonius Kappa CCD area detector diffractometer using graphite-monochromated Mo Kα radiation. Semiempirical absorption corrections based on equivalent reflections were applied.

With the exception of $[Pb_2(L)](ClO_4)_2 \cdot 2MeCN$, where the structure was solved using heavy atom methods, all the structures were solved by direct methods.[25] The structures were completed by iterative cycles of full-matrix least-squares refinement and ΔF syntheses. All non-H atoms, except for those in disordered groups, were refined anisotropically. All H atoms were placed in calculated positions and refined using a riding model.[26] The H atoms on the water molecules in $[H_8L](ClO_4)_6 \cdot 8H_2O$ were not located. Two of the oxygen atoms [O(7) and O(8)] in one perchlorate anion in $[H_8L](ClO_4)_6 \cdot 8H_2O$ were each found to be equally disordered over two sites. In $[Zn_2(HL)](ClO_4)_3 \cdot {}^1/_2MeCN$, one H atom was located in a difference map lying between the two symmetry-related phenolic oxygens of the ligand; this situation was modeled as two mutually exclusive half-occupied positions for the H atom involved, which was restrained to lie 0.82(1) Å from O(22). One of the three perchlorate anions in $[Zn_2(HL)](ClO_4)_3 \cdot {}^1/_2MeCN$ was found to be disordered across a crystallographic inversion center. The disorder was modeled by two independent, half-occupied positions for each of the two unique oxygen atoms. During refinement, appropriate restraints were also applied to the B−F distances and F−B−F angles in $[Cu_2(L)](BF_4)_2 \cdot {}^1/_2MeCN$, and to the Cl−O distances and O−Cl−O angles in the other structures.

Results and Discussion

Synthesis and X-ray Structural Analysis of H_2L. Attempts to prepare metal-free compartmental ligands by reaction of 2,6-diformyl-4-substituted phenols with 1,*n*-diamines under a variety of conditions and in a variety of solvents generally fail to afford the required cyclized ligand. However, the direct [2 + 2] Schiff-base condensation of 1 molar equiv of 1,4-bis(2-aminoethyl)-1,4,7-triazacyclononane (**III**) with 1 molar equiv of 2,6-diformyl-4-methylphenol in MeOH affords, after partial removal of the solvent and addition of petroleum ether, the cofacial macropolycycle H_2L^1 in 82.6% yield as demonstrated by ^{1}H and ^{13}C NMR spectroscopy, and FAB mass spectrometry (Scheme 2).[16,27] Ligand **III** was synthesized in overall 88% yield by reaction of 1-(*p*-tolylsulfonyl)-1,4,7-triazacyclononane (**I**) with 2 equiv of *N*-(*p*-tolylsulfonyl)-aziridine, with subsequent detosylation of the resulting product **II** using concentrated sulfuric acid. The reduction of H_2L^1 was achieved in 70% yields using a mixture of sodium cyanoborohydride and sodium borohydride in MeOH to give $H_2L \cdot 4H_2O$.

Light yellow platy crystals corresponding to the formulation $[H_8L](ClO_4)_6 \cdot 8H_2O$ were grown by slow evaporation of an aqueous solution of $H_2L \cdot 4H_2O$ saturated with $NaClO_4$ and containing a drop of concentrated $HClO_4$. An X-ray structure determination confirmed the formation of the cation $[H_8L]^{6+}$, which lies across a crystallographic inversion center and has all six secondary N-donors protonated (Figure 1). The intramolecular distances and angles are typical of this type of ionophore and the crystal packing involves extensive hydrogen bonds between the perchlorate counteranions, the water molecules, the protonated secondary amines, and the phenolic OH groups. The tertiary amines of the [9]aneN_3 moieties and the secondary amines adjacent to the benzyl

(24) Cosier, J.; Glazer, A. M. *J. Appl. Crystallogr.* **1986**, *19*, 105−107.
(25) Sheldrick, G. M. *Acta Crystallogr., Sect. A* **1990**, *46*, 467−473.
(26) Sheldrick, G. M. *SHELXL-97*; Universität Göttingen: Göttingen, Germany, 1997.
(27) Tei, L.; Blake, A. J.; Wilson, C.; Schröder, M. *J. Chem. Soc., Dalton Trans.* **2002**, 1247−1249.

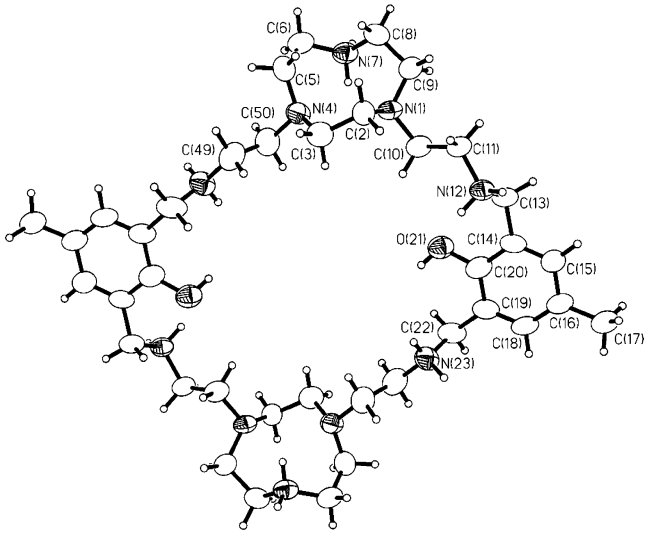

Figure 1. View of the $[H_8L]^{6+}$ cation in $[H_8L](ClO_4)_6 \cdot 8H_2O$ with the numbering scheme adopted. Perchlorate anions and water molecules have been omitted for clarity. Displacement ellipsoids are drawn at 50% probability.

Table 2. Protonation constants of H_2L (298.1 K, 0.1 M Me_4NCl)

reaction	log *K*
$L^{2-} + 2H^+ \rightleftharpoons H_2L$	21.9(2)
$H_2L + H^+ \rightleftharpoons [H_3L]^+$	10.9(1)
$[H_3L]^+ + H^+ \rightleftharpoons [H_4L]^{2+}$	10.4(1)
$[H_4L]^{2+} + H^+ \rightleftharpoons [H_5L]^{3+}$	9.0(1)
$[H_5L]^{3+} + H^+ \rightleftharpoons [H_6L]^{4+}$	7.9(1)
$[H_6L]^{4+} + H^+ \rightleftharpoons [H_7L]^{5+}$	5.7(1)
$[H_7L]^{5+} + H^+ \rightleftharpoons [H_8L]^{6+}$	4.5(1)
$[H_8L]^{6+} + H^+ \rightleftharpoons [H_9L]^{7+}$	1.8(1)

rings are approximately coplanar, with the two aromatic rings located above and below this plane and almost parallel to it. The distances between the centers of the two [9]aneN_3 cavities and the centers of the phenolic rings are 8.27 and 9.09 Å, respectively, affording an approximately square macrocyclic cavity for $[H_8L]^{6+}$. Despite these dimensions, only two water molecules sit within the macrocyclic cavity of $[H_8L]^{6+}$ in $[H_8L](ClO_4)_6 \cdot 8H_2O$; all the other water molecules and the perchlorate anions lie outside the ring cavity.

Ligand Protonation. Ligand protonation was studied by means of potentiometric and UV spectrophotometric measurements, and the results are summarized in Table 2 and Figure 2. H_2L binds up to seven protons in the pH range 2.5−10.5. Two further equilibria, relative to ligand deprotonation ($H_2L \rightleftharpoons HL^- + H^+$ and $HL^- \rightleftharpoons L^{2-} + H^+$), take place at pH > 10.5. In this case, however, the potentiometric measurements do not permit the calculation of protonation constant for a single protonation step, probably due to the two protonation constants being almost equal, and only the global constant relative to the equilibrium $L^{2-} + 2H^+ \rightleftharpoons H_2L$ was determined (log K = 21.9, Table 2).

The most interesting findings in Table 2 are the remarkably high values of the first four basicity constants (>10 log units). It is known that the protonation constants of *p*-cresolate groups are generally higher than 10 log units,[28] thus suggesting that two of the first four protonation steps of the ligand involve the two *p*-cresol functions. On the other hand,

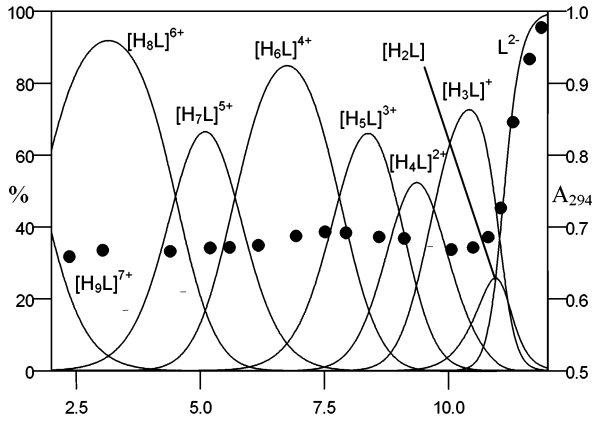

Figure 2. Absorbance at 294 nm (●) and distribution curves of the protonated forms of the ligand H_2L (—) as a function of pH (298.1 K, 0.1 M Me_4NCl, $[H_2L] = 1.6 \times 10^{-4}$ M).

as observed for phenol or *p*-cresol alone, deprotonation of the Ar−OH group gives rise to a 12 nm red-shift of the UV band from 282 nm (ϵ = 4490 dm^3 mol^{-1} cm^{-1} at pH 9) to 294 nm, accompanied by a marked increase of the absorbance (ϵ = 5950 dm^3 mol^{-1} cm^{-1} at pH 12). As shown in Figure 2, this occurs with the formation of the deprotonated species L^{2-} above pH 10.8, indicating that the first two protonation equilibria in Table 2 involve the *p*-cresol functions. In polyamine macrocycles containing one or two phenol groups, protonation of phenolate functions generally takes place among the first protonation steps.[11−13,29] In some cases, however, it has been found that the third or fourth equilibrium involves protonation of phenolate groups with the ligands in zwitterionic forms. For instance, in the case of the two macrocycles 1,4,7,10-tetraaza[12](2,6)phenolphane (HL^2) and 1,4,7,10,13-pentaaza[15](2,6)phenolphane (HL^3) (Scheme 3), which contain respectively, a tetraamine and a pentaamine chain linking the 2,6 positions of a single phenol group, protonation of the phenolate function occurs as the fourth protonation step, due to the involvement of the phenolate group in the stabilization, via H-bonding, of the acidic protons bound to vicinal ammonium groups.[29] In our case, the particular molecular topology of L^{2-} and its high flexibility probably do not allow hydrogen bond interactions between the *p*-cresolate unit and the amine groups, leading to a different protonation pattern and to the existence of H_2L in solution in its non-zwitterionic form. The basicity of H_2L, instead, seems to be parallel to that observed for the ditopic macrocycle 3,6,9,17,20,23-hexaaza-29,30-dihydroxy-13,27-dimethyl-tricyclo[23,3,1^{11,15}]triaconta-1(28),11,13,15(30),25,-26-hexaene (H_2L^4, Scheme 3),[11] which contains two triamine subunits linked by two *p*-cresol moieties. In this case, the first two protonation steps of $[L^4]^{2-}$ involve the Ar−O^- groups.[11] The fact that in both L^{2-} and $[L^4]^{2-}$ the Ar−O^- groups are more basic than amine groups is probably related to the enhanced basicity of the *p*-cresolate group with respect

(28) Smith, R. M.; Martell, A. E. *NIST Stability Constants Database*, version 4.0; National Institute of Standards and Technology: Washington, DC, 1997.
(29) Dapporto, P.; Formica, M.; Fusi, V.; Micheloni, M.; Paoli, P.; Pontellini, R.; Romani, P.; Rossi, P. *Inorg. Chem.* **2000**, *39*, 2156−2163.

Scheme 3

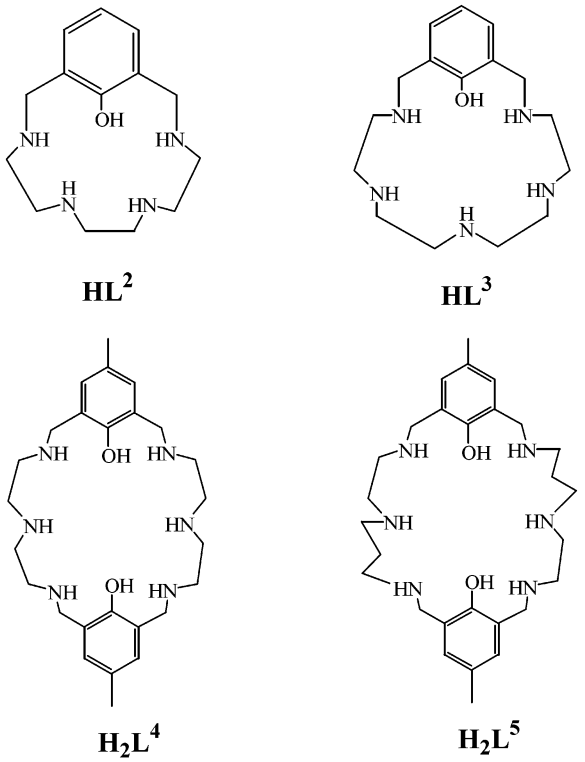

to phenolate one,[28] due to the σ-donating properties of the methyl group in the former. Interestingly, Schröder and coworkers have reported the X-ray crystal structure of the PF_6^- salt of a structural analogue of H_2L^4 (Scheme 3) having two diimino-(*p*-cresol) fragments linked by $-CH_2CH_2-$ bridges in which the two *p*-cresolate groups are H-bonded to the vicinal protonated imine nitrogens.[8]

For L^{2-}, the third and fourth protonation steps take place on amine groups. The values found for these protonation equilibria are higher than those generally found for secondary and tertiary amine groups but are not unusual for a macropolycyclic amine, where the acidic protons can be encapsulated within the macrocyclic cavity and participate in stabilizing hydrogen-bond networks.[30] The similar values of these two protonation constants suggest that the third and fourth protonation steps occur on the two separated 1,4-bis-(2-aminoethyl)-1,4,7-triaazacyclononane units. Similar considerations apply to subsequent protonation equilibria, leading to the conclusion that in the cationic species $[H_8L]^{6+}$ the six positively charged ammonium groups are equally distributed between the two pentaamine compartments of the ligand. Thus, $[H_8L]^{6+}$ contains six NH_2^+ functions separated by an unprotonated amine group. Such a disposition would reduce the electrostatic repulsion between the charged ammonium functions. This suggestion is corroborated by the crystal structure of $[H_8L](ClO_4)_6 \cdot 8H_2O$, which shows protonation of all six secondary amines in the ligand H_2L. The further protonation steps occur on amine groups adjacent to already protonated nitrogens, thus increasing the electrostatic repulsion between the NH_2^+ groups and decreasing the stability of the corresponding protonated species. The low value of the ninth protonation constant of L^{2-} (log $K = 1.8$, see Table 2) and the fact that further protonation steps are not observed in the pH range investigated support the proposed proton distribution.

Metal Complexation in Aqueous Solution. Although complexation in aqueous solution of transition and post transition metals by polyamine ligands incorporating phenol functions has been widely investigated,[11−13,28,31] very little data are available on the stability in aqueous solutions of complexes with ligands displaying a macropolycyclic structure.[32] The particular molecular architecture of H_2L, in which the 1,4-bis(2-aminoethyl)-1,4,7-triaazacyclononane moieties are linked by two *p*-cresol units, prompted us to carry out a potentiometric study of the complexation of Cu^{II}, Zn^{II}, Cd^{II}, and Pb^{II} (Figure 3). The stability constants of the complexes, determined in aqueous solutions containing 0.1 M Me_4NCl, are reported in Table 3. The potentiometric measurements were generally carried out in the pH range 2.5−11; in the case of Pb^{II} the pH range investigated was 2.5−7.5, as the complex would precipitate from alkaline solutions. The ligand shows a similar coordination behavior toward the different metal ions, giving rise to stable mono- and binuclear metal complexes.

The mononuclear species [M(L)] (M = Cu^{II}, Zn^{II}, Cd^{II}, or Pb^{II}) forms several protonated complexes in aqueous solution (Table 3). The complex [Pb(L)] can bind up to four protons, while the remaining mononuclear complexes can also form pentaprotonated species. The protonation constants for the complexes [M(L)] are generally high, the first three protonation constants being only 1−2 log units lower than the corresponding basicity constants of H_2L alone (see Tables 2 and 3). High values for the protonation constants of metal complexes are usually ascribed to protonation of uncoordinated donor atoms which are remote from the metal center. This behavior is typical of ditopic polyamine macrocycles, which display two well-separated binding sites. In other words, in the complexes [M(L)] the metal resides in one of the two 1,4-bis(2-aminoethyl)-1,4,7-triaazacyclononane moieties, while the other, which is not involved in binding to the metal, can be readily protonated. Unfortunately, the presence in solution of both mono- and binuclear complexes, which are formed even with a metal to ligand molar ratio of 1:1, does not allow a reliable spectroscopic characterization of these mononuclear complexes. However, the present complexes [M(L)] are much more stable than the corresponding complexes with 1,4-bis(2-aminoethyl)-1,4,7-triazacyclononane (**III**); for example, log $K = 30.1$ and 23.8 for the Cu^{II} complexes with L^{2-} and with **III**, respectively.[33]

(30) Bencini, A.; Bianchi, A.; Garcia-España, E.; Micheloni, M.; Ramirez, J. A.; *Coord. Chem. Rev.* **1999**, *188*, 97−156.

(31) Guerriero, P.; Tamburini, S.; Vigato, P. A. *Coord. Chem. Rev.* **1995**, *139*, 17−243.

(32) To our knowledge, the stability data for metal coordination by macropolycycles are very rare and limited to small, lithium-selective aza-cryptands: (a) Dapporto, P.; Formica, M.; Fusi, V.; Giorgi, L.; Micheloni, M.; Pontellini, R.; Paoli, P.; Rossi, P. *Eur. J. Inorg. Chem.* **2001**, 1763−1774. (b) Micheloni, M.; Formica, M.; Fusi, V.; Romani, P.; Pontellini, R.; Dapporto, P.; Paoli, P.; Rossi, P.; Valtancoli, B. *Eur. J. Inorg. Chem.* **2000**, 51−57.

(33) Tei, L.; Bencini, A.; Blake, A. J.; Lippolis, V.; Perra, P.; Valtancoli, B.; Wilson, C.; Schröder, M. *J. Chem. Soc., Dalton Trans.*, submitted.

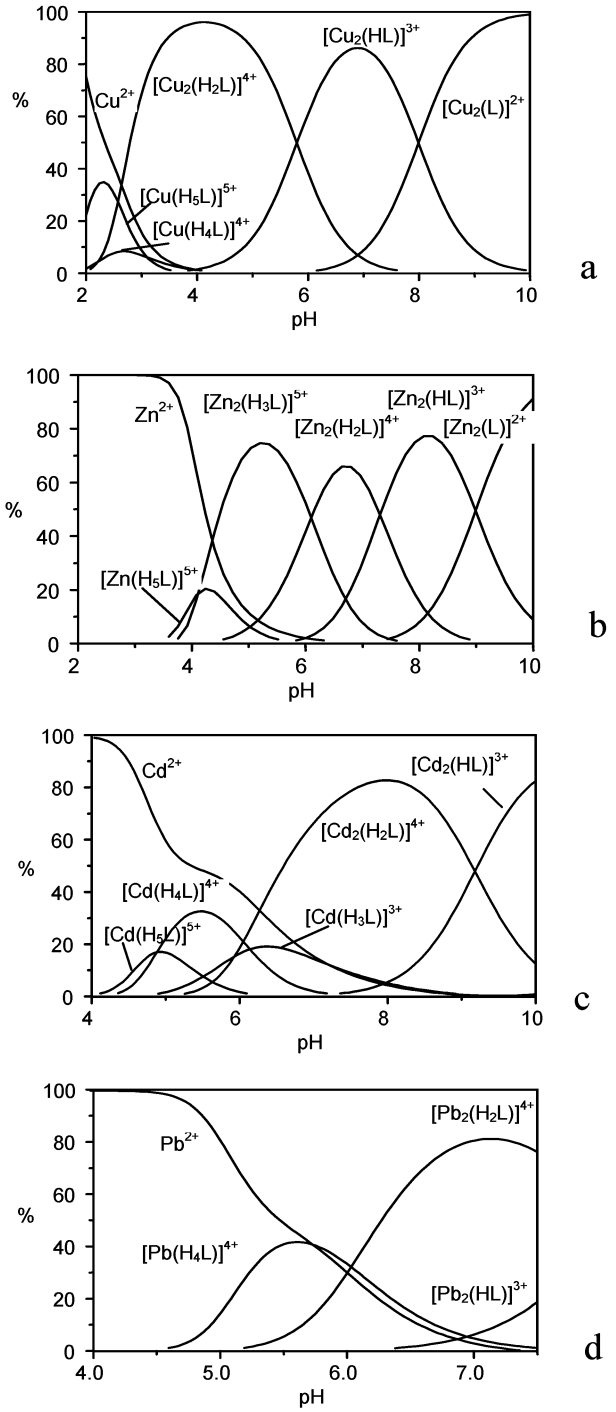

Figure 3. Distribution diagram for the M^{II}/H_2L systems with M = Cu (a), Zn (b), Cd (c), and Pb (d). (Ligand to metal 1:2 molar ratio, $[H_2L] = 1.0 \times 10^{-3}$ M, $M^{II} = 2.0 \times 10^{-3}$ M, 298.1 K, 0.1 M Me_4NCl.)

At the same time, the present mononuclear complexes [M(L)] are far more stable than the corresponding complexes with the ditopic macrocycles 3,6,9,17,20,23-hexaaza-29,30-dihydroxy-13,27-dimethyl-tricyclo[23,3,$1^{11,15}$]triaconta-1(28),11,13,15(30),25,26-hexaene (H_2L^4) and 3,6,10,18,22,25-hexaaza-31,32-dihydroxy-14,29-dimethyl-tricyclo[25,3,$1^{11,17}$]dotriaconta-1(30),12,14,16(32),27,28-hexaene (H_2L^5) (Scheme 3),[11,12] each of which contains two triamine moieties linked by two *p*-cresol units. In the mononuclear complexes with these latter ligands, it has been proposed that deprotonated *p*-cresol functions are involved in metal coordination. The remarkably higher stability of [M(L)] may suggest that, together with the larger number of nitrogen donors available for metal binding, the involvement of deprotonated *p*-cresol functions in metal coordination also contributes to the stabilization of the mononuclear [M(L)] species.

Table 3. Stability Constants of the H_2L Complexes with Cu^{II}, Zn^{II}, Cd^{II}, and Pb^{II} (298.1 K, 0.1 M Me_4NCl)

reaction	Cu^{II}	Zn^{II}	Cd^{II}	Pb^{II}
$M^{2+} + L^{2-} \rightleftharpoons ML$	30.1(1)	20.2(1)	19.7(1)	18.0(1)
$ML + H^+ \rightleftharpoons [M(HL)]^+$	10.4(1)	10.7(1)	10.1(1)	9.6(1)
$[M(HL)]^+ + H^+ \rightleftharpoons [M(H_2L)]^{2+}$	9.3(1)	9.6(1)	9.0(1)	9.5(1)
$[M(H_2L)]^{2+} + H^+ \rightleftharpoons [M(H_3L)]^{3+}$	8.0(1)	8.5(1)	8.8(1)	8.3(1)
$[M(H_3L)]^{3+} + H^+ \rightleftharpoons [M(H_4L)]^{4+}$	5.9(1)	6.3(1)	6.1(1)	7.4(3)
$[M(H_4L)]^{4+} + H^+ \rightleftharpoons [M(H_5L)]^{5+}$	3.1(1)	5.2(1)	4.9(1)	
$ML + M^{2+} \rightleftharpoons [M_2(L)]^{2+}$	18.0(1)	12.3(1)		
$[M_2(L)]^{2+} + H^+ \rightleftharpoons [M_2(HL)]^{3+}$	8.0(1)	9.0(1)		
$2M^{2+} + L^{2-} + H^+ \rightleftharpoons [M_2(HL)]^{3+}$			35.3(1)	35.5(1)
$[M_2(HL)]^{3+} + H^+ \rightleftharpoons [M_2(H_2L)]^{4+}$	5.8(1)	7.3(1)	9.2(1)	8.1(1)
$[M_2(H_2L)]^{4+} + H^+ \rightleftharpoons [M_2(H_3L)]^{5+}$		6.1(1)		

As usually found with ditopic macrocyclic ligands, the mononuclear complexes show a marked tendency to encapsulate a second metal ion in aqueous solutions, to give stable binuclear complexes. For all the systems investigated, binuclear species are largely prevalent from slightly acidic to alkaline pH values in aqueous solutions containing the ligand and the metal ion in 1:2 molar ratio (Figure 3). Protonated mononuclear complexes are only present at acidic pH, and then only in low concentrations.

In the case of Cu^{II} and Zn^{II}, the formation of the binuclear complexes $[M_2(H_2L)]^{4+}$ with the neutral ligand H_2L at slightly acidic pH is followed by deprotonation of the Ar−OH functions in neutral or weakly basic solutions to give the species $[M_2(HL)]^{3+}$ and $[M_2(L)]^{2+}$, respectively. Deprotonation of the *p*-cresol groups is confirmed by analysis of the UV spectra of the complexes recorded at different pH values. As already observed for the deprotonation of the H_2L ligand alone, the formation of the deprotonated complexes $[M_2(HL)]^{3+}$ and $[M_2(L)]^{2+}$ is accompanied by a red shift of the UV band of the *p*-cresol group (ca. 7 nm) and by a simultaneous increase of the molar absorbance. For instance, in the case of the Zn^{II} complexes, the UV band at 285 nm for $[Zn_2(H_2L)]^{4+}$ (pH 6.3) shifts to 292 nm upon formation of the $[Zn_2(L)]^{2+}$ species at pH 10.5. The pH dependence of the absorbance at 292 nm for the Zn^{II}/H_2L system is illustrated in Figure 4; comparison of the UV data points with the distribution curves of the binuclear Zn^{II} complexes shows a clear increase of the absorbance upon the formation of the two deprotonated species $[Zn_2(HL)]^{3+}$ and $[Zn_2(L)]^{2+}$. The most interesting finding is the extremely facile deprotonation of the *p*-cresol functions, which occurs, in the absence of metal cations, only at strongly alkaline pH (see above). The first deprotonation process takes place in slightly acidic solution in the case of the Cu^{II} complex ($pK_a = 5.8$ for the equilibrium $[Cu_2(H_2L)]^{4+} \rightleftharpoons [Cu_2(HL)]^{3+} + H^+$), and at almost neutral pH in the case of Zn^{II} complex ($pK_a = 7.3$ for the equilibrium $[Zn_2(H_2L)]^{4+} \rightleftharpoons [Zn_2(HL)]^{3+} + H^+$). The second deprotonation process occurs at slightly alkaline pH, with pK_a values of 8.0 and 9.0 for the equilibria $[Cu_2(HL)]^{3+} \rightleftharpoons [Cu_2(L)]^{2+} + H^+$ and $[Zn_2(HL)]^{3+} \rightleftharpoons [Zn_2(L)]^{2+} + H^+$,

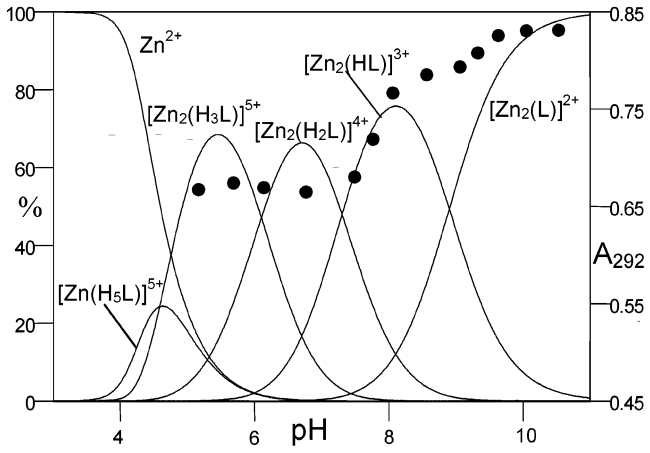

Figure 4. Absorbance at 292 nm (●) and distribution curves of the Zn^{II} complexes (—) as a function of pH (298.1 K, 0.1 M Me_4NCl, $[H_2L] = 1.6 \times 10^{-4}$ M, $[Zn^{II}] = 3.2 \times 10^{-4}$ M).

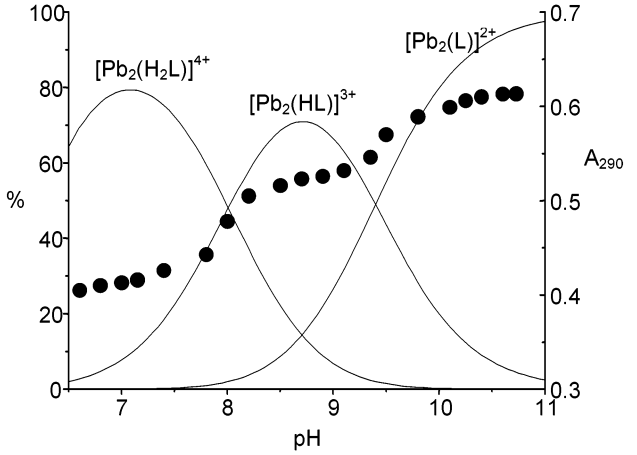

Figure 5. Absorbance at 290 nm (●) of the Pb^{II} complexes with H_2L and distribution curves of the dinuclear Pb^{II} complexes (calculated on the basis of the pK_a values derived from spectrophotometric measurements, —) as a function of pH (298.1 K, 0.1 M Me_4NCl, $[H_2L] = 4.8 \times 10^{-5}$ M, $[Pb^{II}] = 9.6 \times 10^{-5}$ M).

respectively. Such behavior is indicative of a metal-assisted deprotonation process; i.e., the formation of the $[M_2(HL)]^{3+}$ and $[M_2(L)]^{2+}$ complexes implies that the Ar−OH functions simultaneously undergo deprotonation and binding to the metal ions. This feature is confirmed by the crystal structure of the complex $[Cu_2(L)]^{2+}$, which shows both the *p*-cresol groups in the deprotonated form, each strongly interacting with one Cu^{II} ion, and by the structure of the $[Zn_2(HL)]^{3+}$ complex in which only one of the two *p*-cresol groups is deprotonated (see below).

The binuclear Cd^{II} complex shows a somewhat different behavior. As shown in Figure 3c, the formation of the first deprotonated species, $[Cd_2(HL)]^{3+}$, takes place above pH 8 (pK_a = 9.2), while the formation of the completely deprotonated complex $[Cd_2(L)]^{2+}$ is not observed in the pH range investigated (2.5−10.5). Given the softer and less acidic nature of the Cd^{II} ion, it is not surprising that it behaves differently from Zn^{II}. However, the formation of $[Cd_2(HL)]^{3+}$ is again accompanied by a 6 nm red shift in the UV band of *p*-cresol and by an increase of the absorbance, indicating that deprotonation of the phenolic group has accompained metal complexation.

Coordination of Pb^{II} by H_2L was investigated only in the pH range 2.5−7.5: under the conditions used for potentiometric measurements (ligand and metal concentrations 1.0×10^{-3}−2.0×10^{-3} M), the Pb^{II} complex precipitates from alkaline solutions. In the lower pH range, only a small amount of the binuclear species $[Pb_2(HL)]^{3+}$ is formed. We sought therefore to study the deprotonation processes for the species $[Pb_2(H_2L)]^{4+}$ by recording UV spectra at different pH values. The UV spectrum at pH 7, where the protonated binuclear complex $[Pb_2(H_2L)]^{4+}$ is the predominant species in solution (see Figure 3d), displays a band at 282 nm. Once again, a red shift is observed with increasing pH, with $\lambda_{max} = 290$ at pH 10: Figure 5 illustrates the pH dependence of the absorbance at 290 nm in the pH range 6−10.8. Interestingly, two distinct increases in the absorbance can be identified in the pH ranges 7−8.5 and 9−10.5, respectively, and these can be attributed to the two successive deprotonation steps of the $[Pb_2(H_2L)]^{4+}$ complex to give the species $[Pb_2(HL)]^{3+}$ and $[Pb_2(L)]^{2+}$. pK_a values of 8.0± 0.1 and 9.5 ± 0.1 for the equilibria $[Pb_2(H_2L)]^{4+} \rightleftharpoons [Pb_2(HL)]^{3+} + H^+$ and $[Pb_2(HL)]^{3+} \rightleftharpoons [Pb_2(L)]^{2+} + H^+$, respectively, were obtained by treatment of the spectrophotometric data with the HYPERQUAD program.[22] The value of the first deprotonation constant is equal, within the experimental error, to that found by means of potentiometric measurements (8.1 ± 0.1 log units, Table 3).

Crystal Structures of $[Cu_2(L)](BF_4)_2 \cdot {}^1/_2$MeCN (1), $[Zn_2(HL)](ClO_4)_3 \cdot {}^1/_2$MeCN (2), and $[Pb_2(L)](ClO_4)_2 \cdot 2$MeCN (4). The complexation ability of H_2L toward Cu^{II}, Zn^{II}, Cd^{II}, and Pb^{II} was also investigated in the solid state. Binuclear complexes corresponding to the formulation $[Cu_2(L)](BF_4)_2 \cdot {}^1/_2$MeCN (**1**), $[Zn_2(HL)](ClO_4)_3 \cdot {}^1/_2$MeCN (**2**), $[Cd_2(L)](NO_3)_2 \cdot 2$MeCN (**3**), and $[Pb_2(L)](ClO_4)_2 \cdot 2$MeCN (**4**) were obtained in good yields from the reaction of H_2L with the appropriate metal salt in MeCN at room temperature. Crystals suitable for X-ray diffraction analysis were obtained for **1**, **2**, and **4** by slow diffusion of Et_2O vapor into MeCN solutions of the microcrystalline products.

A single-crystal X-ray structure determination on the binuclear complex $[Cu_2(L)](BF_4)_2 \cdot {}^1/_2$ MeCN (**1**) shows each Cu^{II} ion bound to an N_4O donor set within a slightly distorted square-based pyramidal environment (Figure 6, Table 4). For each metal ion, the basal positions of the pyramidal coordination sphere are occupied by the two tertiary N-donors of the [9]aneN_3 moiety [Cu−N 2.016(12)−2.102(12) Å], by one secondary N-donor from the aliphatic chain of the macropolycyclic ligand [Cu−N 2.008(12), 2.008(13) Å], and by one *p*-cresolate oxygen [Cu−O 1.909(9), 1.910(9) Å]. The two metal centers [Cu(1) and Cu(2) in Figure 6], are displaced out of the mean N_3O coordination planes by 0.090 and 0.110 Å for Cu(1) and Cu(2), respectively, in the direction of the apical secondary N-donors N(7) and N(32), respectively [Cu−N 2.283(10) 2.312(11) Å]. The overall N_5O coordination around each metal center is completed by a long interaction involving the remaining two secondary N-donors of the anionic macropolycyclic ligand L^{2-} [Cu(1)−N(12)

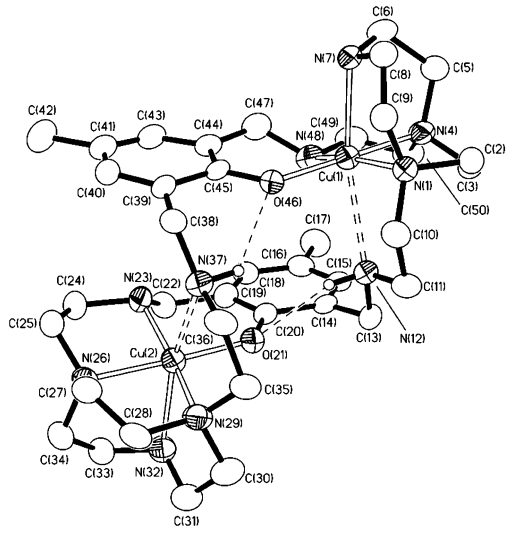

Figure 6. View of the $[Cu_2(L)]^{2+}$ complex cation in **1** with the numbering scheme adopted. The BF_4^- anions and the hydrogen atoms not involved in hydrogen bonding have been omitted for clarity. Displacement ellipsoids are drawn at 30% probability.

Table 4. Selected Bond Lengths (Å) and Angles (deg) for $[Cu_2(L)](BF_4)_2 \cdot {}^1/_2MeCN$ (**1**)

Cu(1)−N(1)	2.102(12)	Cu(2)−N(23)	2.008(12)
Cu(1)−N(4)	2.016(12)	Cu(2)−N(26)	2.043(12)
Cu(1)−N(7)	2.283(10)	Cu(2)−N(29)	2.063(13)
Cu(1)−N(12)	2.597(10)	Cu(2)−N(32)	2.312(11)
Cu(1)−N(48)	2.008(13)	Cu(2)−N(37)	2.593(11)
Cu(1)−O(46)	1.909(9)	Cu(2)−O(21)	1.910(9)
N(1)−Cu(1)−N(4)	85.2(5)	N(23)−Cu(2)−N(26)	86.9(5)
N(1)−Cu(1)−N(7)	81.4(4)	N(23)−Cu(2)−N(29)	166.3(5)
N(1)−Cu(1)−N(12)	75.2(4)	N(23)−Cu(2)−N(32)	106.7(5)
N(1)−Cu(1)−N(48)	167.2(5)	N(23)−Cu(2)−N(37)	95.6(4)
N(1)−Cu(1)−O(46)	97.5(4)	N(23)−Cu(2)−O(21)	91.9(4)
N(4)−Cu(1)−N(7)	82.2(4)	N(26)−Cu(2)−N(29)	85.0(5)
N(4)−Cu(1)−N(12)	99.3(4)	N(26)−Cu(2)−N(32)	80.9(5)
N(4)−Cu(1)−N(48)	86.5(5)	N(26)−Cu(2)−N(37)	97.5(4)
N(4)−Cu(1)−O(46)	177.3(5)	N(26)−Cu(2)−O(21)	178.3(4)
N(7)−Cu(1)−N(12)	156.3(4)	N(29)−Cu(2)−N(32)	82.9(5)
N(7)−Cu(1)−N(48)	107.2(5)	N(29)−Cu(2)−N(37)	74.6(4)
N(7)−Cu(1)−O(46)	98.7(4)	N(29)−Cu(2)−O(21)	95.9(4)
N(12)−Cu(1)−N(48)	96.5(4)	N(32)−Cu(2)−N(37)	157.4(5)
N(12)−Cu(1)−O(46)	81.0(3)	N(32)−Cu(2)−O(21)	100.6(4)
N(48)−Cu(1)−O(46)	90.8(5)	N(37)−Cu(2)−O(21)	81.4(4)

2.597(10) Å, Cu(2)−N(37) 2.593(11) Å, N(7)−Cu(1)−N(12) 156.3(4)°, N(32)−Cu(2)−N(37) 157.4(5)°] (see Figure 6).

The two N_5O-donating compartments of the macropolycycle act, therefore, as isolated donor sets with the *p*-cresolate oxygens not bridging metal ions. In fact, each O-donor is involved in a strong hydrogen bond [H(12)···O(21) 2.31 Å, N(12)−H(12)···O(21) 133°; H(37)···O(46) 2.21 Å, N(37)−H(37)···O(46) 132°] with the secondary N-donor from the adjacent N_5O-donating compartment that weakly interacts with the metal center, thereby forming two $S^1_1(6)$ rings (Figure 6).[34] These intramolecular hydrogen bonds force the donor atoms of the anionic ligand L^{2-} to assume a peculiar disposition with the *p*-cresolate oxygens twisted in opposite directions [twist angle 73.8°] and each pointing toward an individual metal ion. As a result, the *p*-cresolate O-donors cannot bridge the Cu^{II} centers, which are, therefore, segregated within their own N_5O-donor compartments [Cu···Cu distance 5.954 (2) Å]. Interestingly, the mean planes of the two benzene rings of the macropolycycle are almost parallel, but quite distant from each other, with a perpendicular distance of 3.909(4) Å. This might reflect the greater flexibility of L^{2-} as compared to $[L^1]^{2-}$; indeed, in the crystal structure of the binuclear complex $[Cd_2(L^1)](NO_3)_2 \cdot 2MeOH$, the two *p*-cresolate rings are involved in a moderately strong face to face $\pi-\pi$ interaction characterized by a perpendicular distance of 3.342(4) Å between the mean planes of the aromatic rings.[16]

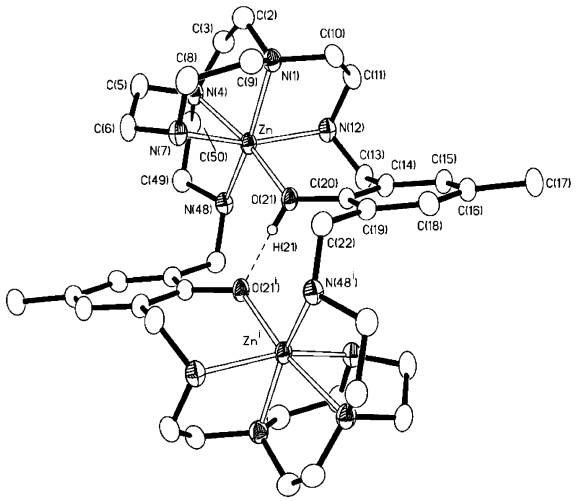

Figure 7. View of the $[Zn_2(HL)]^{3+}$ complex cation in **2** with the numbering scheme adopted. The ClO_4^- anions and the hydrogen atoms not involved in hydrogen bonding have been omitted for clarity. Displacement ellipsoids are drawn at 30% probability (i = 2 − *x*, 2 − *y*, 1 − *z*).

Table 5. Selected Bond Lengths (Å) and Angles (deg) for $[Zn_2(HL)](ClO_4)_3 \cdot {}^1/_2MeCN$ (**2**)

Zn−N(1)	2.194(5)	Zn−N(12)	2.204(4)
Zn−N(4)	2.180(4)	Zn−N(48)	2.179(4)
Zn−N(7)	2.177(4)	Zn−O(21)	2.058(3)
N(1)−Zn−N(4)	82.06(17)	N(4)−Zn−O(21)	170.11(15)
N(1)−Zn−N(7)	80.80(17)	N(7)−Zn−N(12)	159.18(18)
N(1)−Zn−N(12)	79.23(17)	N(7)−Zn−N(48)	107.88(17)
N(1)−Zn−N(48)	159.84(16)	N(7)−Zn−O(21)	90.87(15)
N(1)−Zn−O(21)	101.71(16)	N(12)−Zn−N(48)	92.94(17)
N(4)−Zn−N(7)	80.65(16)	N(12)−Zn−O(21)	87.45(14)
N(4)−Zn−N(12)	102.28(16)	N(48)−Zn−O(21)	96.41(16)
N(4)−Zn−N(48)	81.52(17)		

The single-crystal X-ray structure determination of $[Zn_2(HL)](ClO_4)_3 \cdot {}^1/_2MeCN$ (**2**) reveals the complex cation $[Zn_2(HL)]^{3+}$ lying across a crystallographic inversion center. Each Zn^{II} ion is six-coordinate and bound by an N_5O donor set within a slightly distorted octahedral environment (Figure 7, Table 5). Only one of the two Ar−OH groups of the starting ligand is deprotonated in **2** and is involved in a strong intramolecular hydrogen−bond with the remaining −OH function [O(21)···O(21^i) 2.415(7) Å, i = 2 − *x*, 2 − *y*, 1 − *z*] to form two adjacent $S^1_1(8)$ rings,[34] each of which includes one of the Zn^{II} ions (Figure 7).

Thus, the two N_5O-donating compartments of the macropolyclic anion HL^-, although acting as isolated donor sets, are connected by an unusual Zn−O···H−O−Zn bridge with a Zn···Zn distance of 5.572(1) Å. The intramolecular O(21)−H···O(21^i) hydrogen−bond (Figure 7) and the coordination

(34) Bernstein, J.; Davis, R. E.; Shimoni, L.; Chang, N.-L. *Angew. Chem., Int. Ed. Engl.* **1995**, *34*, 1555−1573.

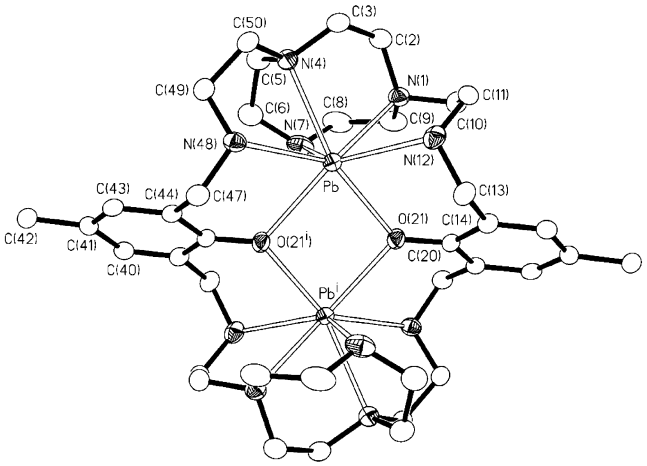

Figure 8. View of the $[Pb_2(L)]^{2+}$ complex cation in **4** with the numbering scheme adopted. The ClO_4^- anions and the hydrogen atoms have been omitted for clarity. Displacement ellipsoids are drawn at 50% probability (i = 1 − *x*, 1 − *y*, 1 − *z*).

Table 6. Selected Bond Lengths (Å) and Angles (deg) for $[Pb_2(L)](ClO_4)_2$·2MeCN (**4**)

Pb−N(1)	2.694(5)	Pb−N(48)	2.744(5)
Pb−N(4)	2.688(5)	Pb−O(21)	2.487(4)
Pb−N(7)	2.586(5)	Pb−O(21^i)[a]	2.630(4)
Pb−N(12)	2.710(5)	Pb−Pb^i	3.9427(5)
N(1)−Pb−N(4)	68.82(15)	N(7)−Pb−N(12)	132.57(17)
N(1)−Pb−N(7)	66.81(17)	N(7)−Pb−N(48)	104.59(17)
N(1)−Pb−N(12)	66.39(16)	N(7)−Pb−O(21)	95.19(16)
N(1)−Pb−N(48)	133.42(14)	N(7)−Pb−O(21^i)	75.10(15)
N(1)−Pb−O(21)	86.67(14)	N(12)−Pb−N(48)	112.67(15)
N(1)−Pb−O(21^i)	137.84(14)	N(12)−Pb−O(21)	74.92(14)
N(4)−Pb−N(7)	67.38(16)	N(12)−Pb−O(21^i)	143.16(14)
N(4)−Pb−N(12)	101.97(15)	N(48)−Pb−O(21)	139.62(14)
N(4)−Pb−N(48)	66.02(14)	N(48)−Pb−O(21^i)	72.58(13)
N(4)−Pb−O(21)	153.84(14)	O(21)−Pb−O(21^i)	79.24(13)
N(4)−Pb−O(21^i)	112.60(13)	Pb−O(21)−Pb^i	100.76(13)

[a] Symmetry operation: i = −*x* + 1, −*y* + 1, −*z* + 1.

sphere around the metal centers force the phenolic groups to assume opposite directions while remaining parallel at a perpendicular distance of 1.655(1) Å.

A single-crystal X-ray structure determination of $[Pb_2(L)](ClO_4)_2$·2MeCN (**4**) shows the complex cation $[Pb_2(L)]^{2+}$ lying across a crystallographic inversion center with two symmetry-equivalent perchlorate counteranions in general positions. The two Pb^{II} centers in the cation lie within the two N_5O donating compartments of L^{2-} and are bridged by the *p*-cresolate oxygen atoms with a short interatomic Pb··· Pb distance of 3.9427(5) Å[35] (Figure 8, Table 6). We can compare the structure of **4** with that of the binuclear complex $[Y_2(L^1)(OH)]^{3+}$ in which the two eight-coordinate Y^{III} ions are bridged not only by the two *p*-cresolate O-donors but also by a hydroxyl group, with the donor atoms evenly distributed about the coordination sphere.[16] In $[Pb_2(L)]^{2+}$ each Pb^{II} is coordinated to seven donor atoms, but some of these bonds are weaker than others: while one *p*-cresolate oxygen [Pb−O(21) 2.487(4) Å] and the secondary N-donor from the [9]aneN_3 moiety [Pb−N(7) 2.586(5) Å] are more strongly bound to the metal center, the other *p*-cresolate oxygen and the remaining N-donors are at longer distances [Pb−O(21^i) 2.630(4) Å, Pb−N 2.688(5)−2.744(5) Å, i = 1 − *x*, 1 − *y*, 1 − *z*]. These structural features, together with the very wide O(21)−Pb−N(48) and O(21^i)−Pb−N(12) angles of 139.62(14)° and 143.16(14)°, respectively, might indicate a stereochemically active $6s^2$ lone pair[36] occupying the region of the coordination hemisphere not encapsulated by the 1,4-bis(2-aminoethyl)-1,4,7-triaazacyclononane moiety. Thus, the coordination sphere at each Pb^{II} center can be tentatively described as a distorted monocapped trigonal prism with the two triangular faces defined by the donors atoms N(4), N(12), N(48) and N(7), O(21), and O(21^i), respectively. The square face capped by N(1) is defined by N(4), N(12), N(7), and O(21).

It is interesting to compare the structures of the three binuclear complexes reported here. On going from **1** to **2**, and to **4**, we observe the ligand gradually adopting a more extended conformation. This can be quantified from the relative disposition of the two *p*-cresolate groups. In **4**, these groups are almost coplanar and face each other, allowing the oxygen donors to be shared between the two metal centers (Figure 8). On going to **1** and **2**, the two *p*-cresolate groups move to occupy parallel planes, approaching a situation in which they are stacked. This movement leads to a gradual segregation of the two metal centers, and is supported by the formation of intramolecular hydrogen bonds involving the phenolate oxygens and the amine donors. An important role is of course played by the stereoelectronic requirements of the metal centers, by their dimensions, and by the flexibility of the large ring ligand.

Conclusions

H_2L^1 and its more flexible reduced form H_2L represent the first examples of phenol-based compartmental macrocycles in which a preformed macrocycle, in particular 1,4,7-triazacyclononane, has been introduced as part of the lateral chains connecting the two phenolic units to afford large binucleating macropolycycles. This may represent a very promising new synthetic approach to the design of binucleating compartmental ligands whose two metal-binding sites are extremely effective in terms of cavity size, geometric requirements, coordination number, and nature of the donor atoms, to selectively form homo- and hetero-binuclear complexes. In fact, by changing the nature of the preformed macrocyclic frameworks symmetrically or asymmetrically introduced within the macropolycyclic structure, selectivity could be reached in the binding properties of the two resulting donating compartments. In our case, stable mono- and binuclear complexes are formed in aqueous solutions, with metal ions being hosted by the 1,4-bis(2-aminoethyl)-1,4,7-triaazacyclononane units of H_2L. In the binuclear complexes, metal-assisted deprotonation of the phenolic groups occurs, depending on the metal, to afford $[M_2(HL)]^{3+}$

(35) (a) Drew, M. G. B.; Rodgers, A.; McCann, M.; Nelson, S. M. *J. Chem. Soc., Chem. Commun.* **1978**, 415−416. (b) Brooker, S.; Kelly, R. J.; Sheldrick, G. M. *J. Chem. Soc., Chem. Commun.* **1994**, 487−488.

(36) (a) Shimoni-Livny, L.; Glusker, J. P.; Bock, C. W. *Inorg. Chem.* **1998**, *37*, 1853−1867. (b) Hancock, R. D.; Shaikjee, M. S.; Dobson, S. M.; Boeyens, J. C. A. *Inorg. Chim. Acta* **1988**, *154*, 229−238.

and $[M_2(L)]^{2+}$ species. Only in the case of large metal ions such as Pb^{II} and Y^{III} are the two metal centers lying within N_5O donating compartments bridged by the phenolate oxygen atoms.

Acknowledgment. We thank the "Regione Autonoma della Sardegna", the Università degli Studi di Cagliari, the Italian Ministero dell'Università e della Ricerca Scientifica e Tecnologica (COFIN 2002), and the University of Nottingham for financial support. We thank the EPSRC-funded Synchrotron Crystallography Service and its director Prof. W. Clegg for collection of single-crystal diffraction data at Daresbury SRS Station 9.8. We wish to thank the EPSRC National Crystallographic Service at the University of Southampton for data collection, and Mr. R. J. Hill for experimental assistance.

Supporting Information Available: Tables giving details of the X-ray crystal structure analyses and crystallographic data in CIF format. This material is available free of charge via the Internet at http://pubs.acs.org.

IC0345065